Published in final edited form as:
Cell Mol Bioeng. 2008 September 1; 1(2-3): 133–145. doi:10.1007/s12195-008-0021-y.

Effect of Electromechanical Stimulation on the Maturation of Myotubes on Aligned Electrospun Fibers

I-Chien Liao, **Jason B. Liu**, **Nenad Bursac**, and **Kam W. Leong**
Department of Biomedical Engineering, Duke University, 136 Hudson Hall, Box 90281, Durham, NC 27708, USA

Abstract

Tissue engineering may provide an alternative to cell injection as a therapeutic solution for myocardial infarction. A tissue-engineered muscle patch may offer better host integration and higher functional performance. This study examined the differentiation of skeletal myoblasts on aligned electrospun polyurethane (PU) fibers and in the presence of electromechanical stimulation. Skeletal myoblasts cultured on aligned PU fibers showed more pronounced elongation, better alignment, higher level of transient receptor potential cation channel-1 (TRPC-1) expression, upregulation of contractile proteins and higher percentage of striated myotubes compared to those cultured on random PU fibers and film. The resulting tissue constructs generated tetanus forces of 1.1 mN with a 10-ms time to tetanus. Additional mechanical, electrical, or synchronized electromechanical stimuli applied to myoblasts cultured on PU fibers increased the percentage of striated myotubes from 70 to 85% under optimal stimulation conditions, which was accompanied by an upregulation of contractile proteins such as α-actinin and myosin heavy chain. In describing how electromechanical cues can be combined with topographical cue, this study helped move towards the goal of generating a biomimetic microenvironment for engineering of functional skeletal muscle.

Keywords

Nanotopography; Tissue engineering; Skeletal muscle; Electromechanical stimulation; Biomimetic microenvironment; Regenerative medicine; Nanofibers

INTRODUCTION

Myocardial infarction affects nearly one million people per year in the United States. The inability of infarcted myocardium to self-repair poses a formidable challenge to successful therapy. Cell-based therapies such as the use of skeletal myoblasts and bone marrow-derived stem cells have been proposed.[21] Both of these cells types are amenable to autologous isolation, *ex vivo* expansion and genetic manipulation before implantation. However, skeletal myoblasts injected at the myocardial infarcted sites and/or at adjacent healthy myocardium can provoke ventricular arrthymia.[5,7] Although some of the injected skeletal myoblasts do develop into skeletal myotubes, they do not electrically couple to the host myocardium. This poor functional integration along with the extensive cell death after implantation has been implicated as one of the culprits of causing arrthymia.[5,7] It has been hypothesized that the application of a pre-developed, mature skeletal muscle cell sheet can satisfy the rigorous myocardium demands better than the injection of single myoblasts.[13,24] This study is therefore motivated by the need to develop more efficient techniques to achieve a mature tissue-engineered skeletal muscle.

Address correspondence to Kam W. Leong, Department of Biomedical Engineering, Duke University, 136 Hudson Hall, Box 90281, Durham, NC 27708, USA. Electronic mail: kam.leong@duke.edu.

Development of mature skeletal myotubes from single myoblasts is a complex process influenced by cell–cell and cell–matrix interactions. Differentiation of myoblasts is governed by cytoskeletal stress originated from the underlying extracellular matrix, causing actin cytoskeleton reorganization and marked activation of stretch-activated ion channels.[1,2,6,17,25,28] Under optimal differentiation conditions, single myoblasts fuse into multinucleated myotubes and mature to synthesize contractile proteins such as myosin, myosin heavy chain, and α-actinin. Mature skeletal fibers are characterized by sarcomeric structures and the ability to undergo repetitive stimulation/contraction.

Development of skeletal myotubes has relied on culture in hydrogel or on patterned surface in the past. In matrigel or fibrin gel scaffold,[11,20,22] skeletal myotubes demonstrate defined sarcomeric structure and are capable of producing tetanus forces ranging from 400 μN to 1 mN. On nanofibers or nano/micro patterned surfaces, skeletal myoblasts elongate and align with the fibers or gratings, producing a tetanus force of up to 500 μN.[3,9,12,15,16,29,30] However, the relationship between myoblast–substrate interaction and subsequent development of sarcomeric structure and production of contractile proteins remains to be elucidated. To further enhance the development of skeletal myotubes, researchers have also proposed the use of mechanical or electrical stimulation during the culture in hydrogels or non-topographical surfaces. Mechanical stimulation increases the mean myotube diameter by 12% as well as the elasticity of the hydrogel-tissue construct.[20] Myotubes developed under mechanical stretch show enhanced production of different isoforms of myosin heavy chain that are characteristic of fast twitch fibers.[23] A stimulation regime that includes cyclic stretch followed by rest upregulates β-integrin expression and activates downstream FAK and RhoA activity, pathways involved in skeletal muscle differentiation.[33] Cyclic electrical pulse can stimulate maturing myotubes to contract and increase their tetanus force.[8,10,27] Low frequency stimulation (1–2 Hz) induces Ca^{2+} transient with improved sarcomere assembly, while higher frequency (10 Hz) fails to induce similar effect.[8]

Hypothesizing that electrical and mechanical cues may further potentiate the topographical effect in enhancing myotube maturation, we studied the culture of skeletal myoblasts on electrospun elastomeric polyurethane fibers with or without synchronized electromechanical stimulation. We observed that aligned fibers enhanced the formation of striated myotubes but have negligible effect on the myotube diameter. Aligned fibers induced stress on the myoblasts as a result of the topography-mediated elongation, thereby upregulating stretch-activation channels, and eventually promoting myotube maturation. The construct responded to electrical stimulation and produced tetanus forces of 1.1 mN with a 10-ms time to tetanus. Under optimal electromechanical stimulation, the differentiated skeletal myoblasts showed a higher degree of striation and upregulation of contractile proteins such as α-actinin and myosin heavy chain compared to those cultured on aligned fibers alone.

MATERIALS AND METHODS

Polyurethane Electrospun Scaffolds and Mechanical Properties

The aliphatic diisocyanate-based polyurethane (PU) fibers (Cardiotech International Inc.) investigated in this study were based on raw materials of two different elastic moduli (80A and 55D). The two polyurethanes have tensile strength of 36 MPa and 62 MPa (elongation at break of 585% and 325%), respectively. Various types of surfaces were fabricated to investigate the effect of topography on skeletal muscle differentiation: film, random oriented or aligned electrospun fibers of varying size (600 nm to 10 μm) and elastic modulus (0.5, 1, and 22 MPa). To fabricate a smooth film surface, the polyurethanes were degassed overnight in 80 °C and molded at 175 °C and 10 MPa for 4 h in a Carver press, followed by cooling at room temperature. To obtain electrospun fibrous mats, the polyurethane pellets were dissolved in a mixed solvent of chloroform and ethanol (75/25 v/v) at various concentrations (7, 10, and 15%

wt/wt) to produce fibers of different diameters. Electrospun fibers of different elastic modulus were produced by using polyurethane pellets of different modulus (80A, 55D and a 50:50 volume ratio blend). The polyurethane solution was dispensed at a flow rate of 3 mL/h through a syringe needle (0.25 mm inner diameter) and exposed to a voltage gradient of 10 kV between the needle and a collecting wheel which served as ground (placed 10 cm from the needle). The collected fibrous mats had a random feature when the wheel was rotating at 1 rpm and an aligned feature at 4000 rpm. A negatively charged needle (−10 kV) was placed over the collecting wheel to enhance the alignment of the electrospun fibers. Electrospinning continued until the electrospun scaffold was at least 50 μm thick, and the scaffold was cut into 1 cm^2 area. Prior to cell culture, the scaffolds were sterilized in ethanol for 1 h and placed under UV light overnight.

The elastic modulus of the aligned electrospun scaffolds was determined according to ASTM protocol (D3822—07). Briefly, each electrospun scaffold was cut into strips of 5 mm wide and 5 cm long and secured in a plastic bracket. The fiber strips were loaded between grips of a dynamic mechanical analysis instrument (RSA III, TA instruments) with a 1-cm gap between the grips. The samples were then strained at a rate of 0.5 mm/min at 22 °C until failure. To determine whether the polyurethane fibers would be able to withstand continuous cyclic loading, the aligned electrospun scaffolds were tested at 10% strain and 1 Hz for 7 days. The changes in stress required to strain the scaffold to 10% can indicate the onset of fatigue. The mechanical properties were determined with a sample size of 20.

Electromechanical Bioreactor Setup/Electromechanical Stimulation Regime

A tubular setup was used to facilitate the synchronized electromechanical stimulation of skeletal myoblasts cultured on aligned nano/microfibers (Fig. 1a). Briefly, aligned electrospun fibrous scaffolds were wrapped around silicone tubings (MPI) that were connected to a 95% O_2/5% CO_2 tank. Figure 1b illustrates the alignment of the electrospun fibers around the silicone tubing, while the insert shows the thickness of the scaffold (~50 μm). The pressure regulator accurately controlled the strain applied to the nanofibers as a result of tubing inflation; at 10 Psi, the aligned fibers experienced strain of 10.6% (Fig. 2a). The solenoid valves connected between the pressure regulator and the bioreactor tubing were used to control the tubing pressure waveform. A computer program (Labview) controlled the closing/opening of the valves, allowing a cyclic strain with controlled frequency and magnitude. A typical stimulation protocol is shown in Fig. 1c, with a repetitive 1-h stimulation at 1 Hz followed by a 5-h rest, between days 2 and 14 post-differentiation. To ensure the mechanical strain reported in the displacement of tubing diameter is the same as the microscopic strain experienced by the cells, 500 nm diameter blue polystyrene microspheres (Polysciences) were added to the surface of the fibers at a concentration of 10^{10} particles/mL/cm^2. Figure 2b shows the corresponding displacement of blue microsphere clusters on fiber-wrapped tubings inflated at different pressures. At 10 Psi, a condition at which the tubing circumference was strained to 10%, the distance between the same two blue microsphere clusters was also increased by 10% (Fig. 2b). In the groups that were exposed to electrical stimulation and synchronized electromechanical stimulation, electrodes were wrapped around the ends of the tubings. Biphasic, 10 ms square pulses of 20 V electrical stimulation (SD9 stimulator, Grass Technologies) were applied with consideration of the necessary rest time. The Labview program was written to synchronize the two stimulation times in order to apply electrical stimulation as the tubing was deflating (500 ms delay from opening of solenoid valves), as illustrated in Fig. 1c. The following electromechanical stimulation protocols were investigated:

1. 5% cyclic strain at 1 Hz starting at 2 days post-differentiation;
2. 10% cyclic strain at 1 Hz starting at 2 days post-differentiation;

3. 5% cyclic strain at 1 Hz starting at 2 days post-differentiation, with a constant 5% pre-stretch applied between cells seeded and the start of cyclic strain;
4. Electrical stimulation was applied at 20 V at 1 Hz starting at day 0, 4 or 7 days post-differentiation;
5. Synchronized stimulation consisted of pre-stretched mechanical stimulation applied in group 3 with electrical stimulation starting at day 7.

Cell Line and Cell Culture

Mouse skeletal myoblasts (C2C12 cell line) were purchased from ATCC and expanded in proliferative medium (Dulbecco's Modified Eagle's Medium (high glucose, Gibco) supplemented with 10% fetal bovine serum (35-015-CV, Mediatech), 10% bovine calf serum (12133C, Sigma), 0.5% chick embryo extract (Accurate chemicals), and 1% penicillin/streptomycin). The undifferentiated myoblasts were maintained below 80% confluency and only passages between 2–4 were used in this study. To differentiate myoblasts into skeletal myotubes, the cells were first seeded onto surfaces of interest at a density of $5 \times 10^5/cm^2$ and maintained in proliferative medium for 5 days. Cells were seed on the tubular surface by placing a sterilized trough under the tubing to contain the added medium for 1 h. The cell-seeded constructs were then shifted into differentiation medium (Dulbecco's Modified Eagle's Medium supplemented with 8% equine serum, SH30074.03, Hyclone, and 1% penicillin/streptomycin) for 14 days. The media were changed every 2 days to ensure sufficient nutrient for myotube formation. Skeletal myoblasts began cytoplasmic fusion at day 2 and formed skeletal myotubes by day 7 of differentiation. Occasional spontaneous contraction was noticeable at day 7 and became more prominent by day 14.

Immunocytochemistry, Cell Elongation, and Alignment Assay

To elucidate the interaction of myoblasts with film or electrospun fibers prior to taking part in myotube formation, the cells were seeded at a density of $5000/cm^2$ and cultured for 2 days. The cells were fixed in 4% paraformaldehyde solution for 1 h, permeated in 0.1% Triton X-100 solution for 30 min and stained with Alexa^{594} phalloidin (Invitrogen) and DAPI to visualize actin filaments and nucleus, respectively. The cell elongation factor (F) was determined by $F = (L - W)/W$, where L = maximum length of cytoplasm, W = maximum width of cytoplasm along the direction perpendicular to the length. The alignment of the cells was determined by measuring the angle difference of individual cells vs. the mean angle of overall cell population. A minimum of 100 cells was measured for each group to achieve statistical significance. To further characterize the anchorage and expression of stretch-activated ion channels of the cells on various surfaces, some of the samples were blocked in 1% goat serum solution for 1 h, and immunostained with rabbit polyclonal paxillin (1:100 dilution, Abcam) or rabbit polyclonal transient receptor potential cation channel-1 (TPRC-1, 1:50 dilution, Sigma) primary antibody. The secondary antibodies and stains used were Alexa^{488} anti-rabbit IgG antibody (1:200 dilution, Invitrogen), DAPI and Alexa^{594} phalloidin (Invitrogen) to visualize nucleus and filamentous actin, respectively. The cell-seeded scaffolds were mounted onto a glass slide and visualized using inverted confocal microscope (LSM 510 Meta with AxioCam HR camera, Carl Zeiss, Thornwood, NY) with 40× and 100× objective lens. The excitation/emission wavelength settings are 488 nm/520–555 nm (FITC), 594 nm/575–615 nm (Rhodamine), and 408 nm/420–480 nm (DAPI).

Fourteen days post-differentiation, cells cultured on various surfaces were fixed, permeated, and blocked as mentioned above. The cells were immunostained for sarcomeric α-actinin (1:100 dilution, EA-53, Abcam) and counterstained with DAPI and Alexa^{488} phalloidin (Invitrogen). The presence of periodic striations, as illustrated by α-actinin staining, was evaluated by examining at least 100 myotubes. In this study, cells showing partial Z bands

were counted as positive for showing striations. The data were presented as a percentage of total myotubes showing striated pattern and expressed as mean ± SD. The diameters of the myotubes were measured using Image-J software.

Western Blot Analysis

At 14 days post-differentiation, cells were rinsed once, and scraped in cell lysis buffer (with 1:10 v/v of protease inhibitor). The cell suspension was shaken at 4 °C for 30 min and the cell lysate was spun down by centrifugation for 3 min. The supernatant was collected and the protein concentration was determined by NanoDropTM 1000 Spectrophotometer (Thermo Scientific). Equal volume of Laemmli sample (with 1:10 v/v of 2-mercaptoethanol) was added to supernatant prior to freezing. The proteins (10 μg) from lysate were separated by SDS-PAGE, electrotransferred to PVDF membrane, blocked in 5% non-fat dry milk containing 0.1% Tween-20 (TTBS) and incubated overnight with various primary antibodies including mouse anti-sarcomeric α-actinin (EA 53, 1:100 dilution, Abcam), mouse anti-fast myosin heavy chain (MY32, 1:500 dilution, Abcam), rabbit anti-desmin (1:50 dilution, Abcam), mouse anti-skeletal muscle troponin I (1:100 dilution, Abcam), mouse anti-myogenin (F5D, 1:200, Abcam), mouse-anti myosin (1:500, Sigma), and mouse-anti GAPDH (1:5000, Abcam). The bound antibodies were detected by anti-mouse or anti-rabbit IgG1 conjugated to horseradish peroxidase (Calbiochem). The proteins were detected by Immuno-Star HRP chemiluminescence (Biorad) and imaged using Alpha Innotech imaging system (FluorChem).

Skeletal Muscle Contractility

The contractility of the skeletal muscle cultured on aligned electrospun fibers was measured using a sensitive force transducer (force detection range: 1 μN to 5 mN, Model 801B, Aurora Scientific). The cell-seeded construct (1 cm^2 area with an estimated thickness of 50 μm) was secured between two needles on the force measurement setup, with one side fixed and other attached to the force transducer. The construct was maintained in differentiation medium at 37 °C for the duration of the study. Electrical pulses (20 V, 10 ms pulse width at 10 and 20 Hz) were applied to measure the tetanus force of the construct, and the average force over three trials was recorded. Baseline force was measured preceding the onset of stimulation. The recorded values were based on three measurements of three different constructs.

Statistical Analysis

Data was analyzed using Student's *t* test (SPSS). A difference with $p < 0.05$ value was considered to be statistically significant and indicated by asterisks. All data are shown as mean ± SEM.

RESULTS

Polyurethane Topography and Mechanical Properties

Figures 3a–f illustrates the different topographical features, ranging from smooth film (a), randomly oriented fibers (b), and aligned fibers (c–e). The aligned fiber diameters ranged from 600 ± 100 nm to 10 ± 4 μm (Fig. 3f). The large size distribution seen in the 10 μm group is typical of the electrospinning technology. Polyurethanes of different stiffness (0.5, 1, and 22 MPa) were electrospun in this study (Fig. 2c). Depending on the composition of the polyurethane used, the electrospun fibers could be stretched up to 300% and with no evidence of fatigue under 10% cyclic loading of 1 Hz over a period of 7 days (Fig. 2d).

Myoblast Differentiation on Various Surface Topographies

When cultured on random fibers, the myoblasts showed no preferred orientation and predominantly exhibited polymorphic shape and round nuclei (Figs. 4a and 4b). In contrast,

aligned fibers guided the cell alignment (> 90% of cells aligned within 10° of the fiber orientation), although fiber diameters between 600 nm to 10 μm produced no statistically significant difference in alignment and cell elongation factor (Figs. 4a–e). On all aligned fibers, myoblasts showed significant cytoplasmic elongation compared to randomly aligned fibers (average elongation factor of 13.15 for aligned vs. 3.7 for random topography) as well as significant elongation of the nucleus. Immunostaining for focal adhesion sites and actin filaments helped elucidate the correlation between cell morphology and cell–substrate interaction. On PU film, myoblasts showed focal adhesion points around the periphery of the cytoplasm, with little orientation in the actin filaments (Fig. 5a). On random fibers, there was an increase in cell and nucleus elongation, associated with the migration of the focal adhesion sites from the periphery towards the nucleus and a slight orientation of actin filaments in the direction of the elongated cytoplasm (Fig. 5b). On aligned fibers, the actin filaments were highly aligned within the elongated cytoplasm and the focal adhesion sites were distributed evenly throughout the cytoplasm (Fig. 5c). Investigation of the expression level of transient receptor potential cation channel-1 (TRPC-1), a subtype of stretch-activated cation channels, provided evidence that the elongation of cells due to aligned topography was a result of stretch induced by the surface. TRPC-1 (illustrated in green in Figs. 5d–f) was progressively activated when myoblasts were cultured on film vs. random vs. aligned fibrous surfaces.

Differentiation of Skeletal Myoblasts Cultured on Various Surface Topographies

This series of experiments screened the surface topography (film, random, and aligned fibers), matrix stiffness (0.5, 1, and 22 MPa), and fiber sizes (600 nm, 2 μm and 10 μm) to identify the optimal surface features that might enhance myoblast differentiation. The presence of sarcomeric structure is an indication of myotube maturation manifested by striated features in the immunostaining of α-actinin. The differentiation of myoblasts on various surfaces was scored by the percentage of myotubes showing cross-striations and the diameter of the myotubes. At 14 days post-differentiation, only 25% of myotubes cultured on film showed striations, vs. 55% on random surface and 70% on aligned surface (Figs. 6a–c, i). On aligned fibers with different matrix stiffness (Figs. 6c–e, i), myotubes showed the highest level of differentiation on the softest polyurethane and progressively lower level as the matrix stiffness increased. Fiber diameters between 600 nm to 10 micron did not make a significant difference in terms of differentiation (Figs. 6c, f, g, i). No significant change in myotube diameter was seen as a result of different surface topographies (Fig. 6h).

Western blot analysis for contractile proteins was consistent with the observation in immunofluorescent images. The production of all contractile proteins (α-actinin, myosin, myosin heavy chain, and troponin I) appeared upregulated as the myoblasts were differentiated on aligned fibers vs. random fibers vs. films (Fig. 7a). Further analysis showed statistically significant upregulation of myogenin, actinin, and myosin (Fig. 7b) when the cells were cultured on aligned fibers. Among different fiber diameter groups, there was no difference in the level of contractile protein production (Figs. 7a and 7b).

Contractile force production analysis of the skeletal myotubes cultured on aligned fibers showed that the tissue constructs were capable of producing a tetanus force of 1.1 mN, with a time to tetanus around 10 ms and a twitch force of 600 μN (Fig. 8). The contractile force recorded from the aligned fibrous tissue construct is comparable to that reported in the literature when myoblasts are differentiated in the hydrogels.[11]

Differentiation of Skeletal Myoblasts Cultured Under Various Stimulation Regimes

When cyclic mechanical stretching (1 Hz for 1 h with 5 h of rest) was applied to the differentiating myoblasts starting at 2 days post-differentiation, the myotubes at day 14 exhibited evidence of overstretching at both 5 and 10% strain (Figs. 9b and 9c). Very few

myoblasts fused to form myotubes on the scaffolds, and those that were present were short and lacked sarcomeric structures. From these groups, total protein production tripled but there were very little contractile proteins such as myosin (data not shown). This suggested that the cells were overstretched and had shifted into a proliferative state as a result of injury. To counteract this injury process, a constant stretch of 5% was applied as the cells were seeded onto the scaffold and maintained until 2 days post-differentiation. We speculated that this would condition the myoblasts to better withstand the cyclic loading applied from days 2–14. Indeed, myoblasts cultured in this manner showed an increased fraction of striated myotubes from 70 to 75% (Fig. 9d). The increase in myotube diameter as a result of cyclic stretching was not statistically significant (Fig. 9i).

Electrical stimulation (20 V, 1 Hz for 1 h with 5 h of rest) was applied at three time points, day 0, 4, and 7 post-differentiation, in order to investigate the effect of electrical stimulation prior to myotube formation (day 0 and 4) compared to that post-myotube differentiation (day 7). Immunofluorescence images (Figs. 9e and 9f) revealed a lower degree of striation when the electrical stimulation was applied prior to myotube formation (10% when starting at day 0, and 45% when starting at day 4). However, when electrical stimulation was applied beginning at day 7, the percentage of myotube showing striation increased from 70 to 85% (Fig. 9g) compared to the unstimulated control. The myotubes contracted in synchrony with the applied electrical stimuli for the duration of the stimulation.

Finally, synchronized electromechanical stimulation was applied to the cells by combining the pre-stretched mechanical stimulation with electrical stimulation beginning at day 7. Electrical stimulation was programmed to be applied with 500 ms delay from the opening of solenoid valves (electrical stimulation was applied as the tubing deflates) and the stimulation regime also included a 5-h rest time after 1 h of stimulation. Myotubes differentiated under this condition showed an increase in percent of myotube striation (70–85%) compared to the unstimulated control (Fig. 9h). There was no statistically significant change in myotube diameter. Western blot analysis of the contractile protein expression was consistent with the findings from confocal analysis. Compared to unstimulated control, myoblasts cultured under synchronized stimulation showed an upregulation of contractile protein production (Fig. 9j). It was unclear if the synchronized stimulation was superior over single stimulation groups in driving the maturation of myotubes, although the protein level of fast myosin heavy chain (Fig. 9j) was found to be significantly higher (not shown).

DISCUSSION

During the development of skeletal myotubes, myoblasts must first upregulate their primary myogenic transcription factors, MyoD and Myf5, followed by the over-expression of secondary myogenic factor such as myogenin and MRF4.[6] The cytoskeletal remodeling and fusion of myoblasts into myotubes require remodeling of the stress fibers, which activate stress-activated channels (SACs) and change the electrical properties of the cells. The activation of SACs triggers Ca^{2+}-dependent signaling cascade such as the phospholipase C and IP_3 pathways, which in turn lead to phenotypic maturation of myoblasts into myotubes.[28] Since this process is closely related to the cell–extracellular matrix interaction, the underlying substrate features can influence the level of myotube maturation. We have demonstrated that topographical cues can play a significant role in the development of skeletal myotubes. The aligned topography of the PU fibers causes a cytoskeleton reorganization of the myoblasts, not only to orient the cells in the direction of the fibers but also to amplify their degree of elongation and fusion. The increased elongation is a result of uniaxial stress in the direction of fiber orientation, as illustrated in the reorganization of focal adhesion sites from the periphery to the center. The upregulation of TRPC-1 expression (one type of SACs) suggests that the effect of aligned

topography on enhanced myotube differentiation may be mediated by Ca^{2+}-dependent signaling pathways.

In addition, we have compared differentiation of myoblasts on fibers of various matrix stiffness, a property shown to modulate the level of skeletal myotube differentiation through cell–substrate interaction.[4] We have observed that myoblasts form myotubes with a higher degree of striation when cultured on softer fibers (0.5 MPa) vs. stiffer fibers (22 MPa). This observation matches the findings of Engler *et al*. but differs in the type of substrate studied (fiber vs. hydrogel) and the stiffness values (0.5 MPa vs. 15 kPa).[4] This study also investigates the effect of fiber size (600 nm to 10 μm) on the differentiation of skeletal myotubes. Topographical features of the substrate, particularly in the submicron range, have been reported to influence the morphology, proliferation, and migration of smooth muscle cells.[32] The topographical cues also affect the differentiation of human mesenchymal cells, where nanogratings in the range of 350 nm to 2 μm width stimulate the upregulation of neuronal genes in a size-dependent manner.[31] In this study, the differentiation of skeletal myoblasts was insensitive to the fiber size within the range of 600 nm to 10 μm (Fig. 6). As the extent of cell elongation was similar among fibers of 600 nm to 10 μm, the differentiating myoblasts may have experienced similar stretch forces and yielded similar levels of differentiation. In general, this study also underscores the importance of mechanical microenvironment in shaping tissue development. However, further studies will have to be performed to understand the underlying mechanism and clarify the relative contributions of substrate stiffness and topography in modulating the differentiation of myoblasts.

The mechanical and electrical stimulation regimes used in this study have been adapted from literature that suggests optimal enhancement of myogenesis. For instance, a typical 5 or 10% strain on cells cultured in matrigel would improve myotube diameter and density in the hydrogel.[20] In this study, when 5 or 10% of cyclic strain was applied to the skeletal myotubes differentiated on aligned fibers, there was a negative effect on myoblast maturation and an evidence of extensive proliferation (Figs. 9b and 9c). Other reports in the literature show that exposure of skeletal myoblasts *in vitro* to strains of lower magnitude (< 10%) enhances differentiation over proliferation, while this pattern is inverted for strains above 15%.[14,18,26] In this study, the highly aligned myoblasts on fibers may have been already pre-stretched and any additional mechanical stretching became deteriorating to their maturation capability. On the other hand, pre-stretched myoblasts (when a 5% strain is maintained from cell seeding to 2 days post-differentiation) benefited from additional cyclic stretching as evidenced by enhanced differentiation and production of contractile proteins (Figs. 9d and 9j). The interesting finding that the alignment of polyurethane fibers may exert a pre-stretch on cells highlights the need to consider carefully the combination of topographical and mechanical stimuli in optimizing myogenesis.

We have also found that the timing of the application of electrical stimulation is a crucial factor in modulating the myoblast differentiation. When stimulation is applied prior to myotube assembly, the cells appear to be incapable of benefiting from the electrical stimulation, resulting in only myotubes of poor sarcomeric structure (Fig. 9e). This finding is consistent with a previous study where skeletal myoblasts are cultured on PGA fibrous scaffolds.[19] On the other hand, electrical stimulation applied after myotube assembly was found to be highly beneficial. Using the optimal mechanical (pre-stretched with 5% cyclic strain) and electrical (20 V at 1 Hz, applied 7 days post-differentiation) stimulation conditions, we have investigated myoblast differentiation under synchronized electromechanical stimulation. While the synchronized stimulation improved the level of striation and contractile protein production compared to unstimulated cells, its benefit over single stimulation (electrical or mechanical) is unclear (Figs. 9h and 9j). Given this is the first report on the coupling of electromechanical stimulation for myotube formation, further systematic studies with different patterns of stimulation would be

required to identify any synergistic effects. A more detailed study on the production of different isotypes of myosin heavy chain, Ca^{2+} homeostasis and contractile force generation in myotubes will be needed to elucidate the potential differences brought about under different synchronized stimulation conditions. The current study sets the experimental framework for combining the topographical with electromechanical cues in further optimization of myogenesis for engineering of functional skeletal muscle.

CONCLUSION

A comprehensive study was conducted on how substrates of various topographical features and electromechanical stimulation could influence the differentiation of skeletal myoblasts into contractile myotubes. Aligned topography induced cell elongation, focal adhesion reorganization, and stretch-activated ion channel upregulation, similar to effects previously observed during application of a constant uniaxial stretch. Stretching without pre-conditioning the myoblasts on aligned fibers resulted in inhibited myotube differentiation and upregulated cell proliferation. This phenomenon could be counteracted by pre-stretching the cells prior to application of cyclic strain, with the resulting myotubes demonstrating enhanced differentiation. Electrical stimulation applied post, but not prior to, myotube formation also enhanced process of myogenesis as evidenced by a higher level of striated myotubes and contractile protein expression. In describing how electromechanical and topographical cues can be combined in modulating the process of myogenesis, this study helps move towards the generation of a biomimetic microenvironment for engineering of functional skeletal muscle tissues.

Acknowledgments

The authors would like to acknowledge the contribution of Dr. George Truskey, Caroline Rhim and Matt Brown. Support by NIH Grants EB003447 to Kam W. Leong and AR055226 to Nenad Bursac are also acknowledged.

References

1. Alisi A, Spaziani A, Anticoli S, Ghidinelli M, Balsano C. PKR is a novel functional direct player that coordinates skeletal muscle differentiation via p38MAPK/AKT pathways. Cell Signal 2008;20:534–542. [PubMed: 18164587]
2. Clark CB, McKnight NL, Frangos JA. Stretch activation of GTP-binding proteins in C2C12 myoblasts. Exp Cell Res 2004;292:265–273. [PubMed: 14697334]
3. Cronin EM, Thurmond FA, Bassel-Duby R, Williams RS, Wright WE, Nelson KD, Garner HR. Protein-coated poly (L-lactic acid) fibers provide a substrate for differentiation of human skeletal muscle cells. J Biomed Mater Res 2004;69A:373–381.
4. Engler AJ, Griffin MA, Sen S, Bonnemann CG, Sweeney HL, Discher DE. Myotube differentiate optimally on substrates with tissue-like stiffness: pathological implications for soft or stiff microenvironments. J Cell Biol 2004;166:877–887. [PubMed: 15364962]
5. Fernandes S, Amirault JC, Lande G, Nguyen J, Forest V, Bignolais O, Lamirault G, Heudes D, Orsonneau J, Heymann M, Charpentier F, Lemarchand P. Autologous myoblast transplantation after myocardial infarction increases the inducibility of ventricular arrhythmias. Cardiovasc Res 2006;69:348–358. [PubMed: 16376327]
6. Formigli L, Meacci E, Sassoli C, Squecco R, Nosi D, Chellini F, Naro F, Fancini F, Zecchi-Orlandini S. Cytoskeleton/stretch-activated ion channel interaction regulates myogenic differentiation of skeletal myoblasts. J Cell Physiol 2007;211:296–306. [PubMed: 17295211]
7. Fouts K, Fernandes B, Mal N, Liu J, Laurita KR. Electrophysiological consequence of skeletal myoblast transplantation in normal and infarcted canine myocardium. Heart Rhythm 2006;3:452–461. [PubMed: 16567294]
8. Fujita H, Nedachi T, Kanzaki M. Accelerated de novo sarcomere assembly by electric pulse stimulation in C2C12 myotubes. Exp Cell Res 2007;313:1853–1865. [PubMed: 17425954]

9. Huang NF, Patel S, Thakar R, Wu J, Hsiao BS, Chu B, Lee RJ, Li S. Myotube assembly on nanofibrous and micropatterned polymers. Nano Lett 2006;6:537–542. [PubMed: 16522058]
10. Huang YC, Dennis RG, Baar K. Cultured slow vs. fast skeletal muscle cells differ in physiology and responsiveness to stimulation. Am J Physiol-Cell Physiol 2006;291:11–17.
11. Huang YC, Dennis RG, Larkin L, Baar K. Rapid formation of functional muscle in vitro using fibrin gels. J Appl Physiol 2004;98:706–713. [PubMed: 15475606]
12. Huber A, Pickett A, Shakesheff KM. Reconstruction of spatially orientated myotubes in vitro using electrospun, parallel microfibre arrays. Eur Cells Mater 2007;14:56–63.
13. Kondoh H, Sawa Y, Miyagawa S, Sakakida-Kitagawa S, Memon IA, Kawaguchi N, Mtsuura N, Shimizu T, Okano T, Matsuda H. Longer preservation of cardiac performance by sheet-shaped myoblast implantation in dilated cardiomyopathic hamsters. Cardiovasc Res 2006;69:466–475. [PubMed: 16423569]
14. Kumar A, Murphy R, Robinson P, Wei L, Boriek AM. Cyclic mechanical strain inhibits skeletal myogenesis through activation of focal adhesion kinase, Rac-1 GTPase, and NF-kappaB transcription factor. FASEB J 2004;13:1524–1535. [PubMed: 15466361]
15. Lam MT, Sim S, Zhu X, Takayama S. The effect of continuous wavy micropatterns on silicone substrates on the alignment of skeletal muscle myoblasts and myotubes. Biomaterials 2006;27:4340–4347. [PubMed: 16650470]
16. Neumann T, Hauschka SD, Sanders JE. Tissue engineering of skeletal muscle using polymer fiber arrays. Tissue Eng 2003;9:995–1003. [PubMed: 14633383]
17. Omoteyama K, Mikami Y, Takagi M. Foxc2 induces expression of MyoD and differentiation of the mouse myoblast cell line C2C12. Biochem Biophys Res Commun 2007;358:885–889. [PubMed: 17506979]
18. Otis JS, Burkholder TJ, Pavlath GK. Stretch-induced myoblast proliferation is dependent on the COX2 pathway. Exp Cell Res 2005;2:417–425. [PubMed: 16168411]
19. Pedrotty DM, Koh J, Davis BH, Taylor DA, Wolf P, Niklason LE. Engineering skeletal myoblasts: roles of three-dimensional culture and electrical stimulation. Am J Physiol-Heart Circ Physiol 2005;288:1620–1626.
20. Powell CA, Smiley BL, Mills J, Vanden-burgh HH. Mechanical stimulation improves tissue-engineered human skeletal muscle. Am J Physiol-Cell Physiol 2002;5:1557–1565.
21. Ramos GA, Hare JM. Cardiac cell-based therapy: cell types and mechanisms of actions. Cell Transplant 2007;16:951–961. [PubMed: 18293894]
22. Rhim C, Lowell DA, Reedy MC, Slentz DH, Zhang SJ, Kraus WE, Truskey GA. Morphology and ultrastructure of differentiating three-dimensional mammalian skeletal muscle in a collagen gel. Muscle Nerve 2007;36:71–80. [PubMed: 17455272]
23. Sakiyama K, Abe S, Tamatsu Y, Ide Y. Effects of stretching stress on the muscle contraction proteins of skeletal muscle myoblasts. Biomed Res 2005;26:61–68. [PubMed: 15889619]
24. Sbrana F, Sassoli C, Meacci E, Nosi D, Squecco R, Paternostro F, Tiribilli B, Zecchi-Orlandini S, Francin F, Formigli L. Role of stress fiber contraction in surface tension development and stretch-activated channel regulation in C2C12 myoblasts. Am J Physiol-Cell Physiol 2008;295:160–172.
25. Siepe M, Giraud MN, Liljensten E, Nydegger U, Menasche P, Carrel T, Tevaearai HT. Construction of skeletal myoblast-based polyurethane scaffolds for myocardial repair. Artif Organs 2007;6:425–433. [PubMed: 17537054]
26. Tatsumi R, Sheehan SM, Iwasaki H, Hattori A, Allen RE. Mechanical stretch induces activation of skeletal muscle satellite cells in vitro. Exp Cell Res 2001;1:107– 114. [PubMed: 11412043]
27. Thelen MH, Simonides WS, van Hardeveld C. Electrical stimulation of C2C12 myotubes induces contractions and represses thyroid-hormone-dependent transcription of the fast-type sacroplasmic-reticulum Ca^{2+}- ATPase gene. Biochem J 1997;321:845–848. [PubMed: 9032474]
28. Woo JS, Kim DH, Allen PD, Lee EH. TRPC3- interacting triadic proteins in skeletal muscle. Biochem J 2008;411:399–405. [PubMed: 18215135]
29. Yamamoto DL, Csikasz RI, Li Y, Sharma G, Hjort K, Karlsson R, Bengtsson T. Myotube formation on micro-patterned glass: intracellular organization and protein distribution in C2C12 skeletal muscle cells. J Histochem Cytochem 2008;10:881–892. [PubMed: 18574252]

30. Yan W, George S, Fotadar U, Tyhovych N, Kamer A, Yost MJ, Price RL, Haggart CR, Holmes JW, Terracio L. Tissue engineering of skeletal muscle. Tissue Eng 2007;13:2781–2790. [PubMed: 17880268]

31. Yim EK, Pang SW, Leong KW. Synthetic nanostructures inducing differentiation of human mesenchymal stem cells into neuronal lineage. Exp Cell Res 2007;9:1820–1829. [PubMed: 17428465]

32. Yim EK, Reano RM, Pang SW, Yee AF, Chen CS, Leong KW. Nanopattern-induced changes in morphology and motility of smooth muscle cells. Biomaterials 2005;26:5405–5413. [PubMed: 15814139]

33. Zhang SJ, Truskey GA, Kraus WE. Effect of cyclic stretch on beta1D-integrin expression and activation of FAK and RhoA. Am J Physiol-Cell Physiol 2007;6:57–69.

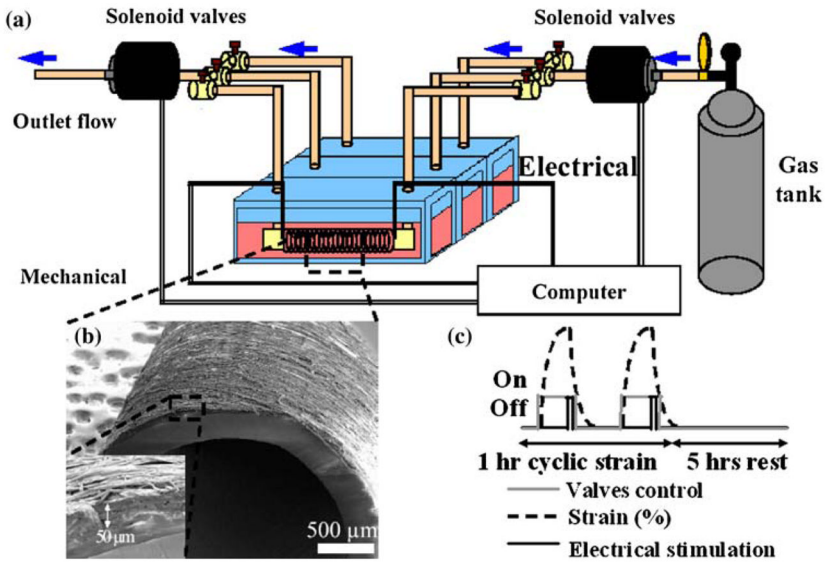

FIGURE 1.

Electromechanical stimulation setup. A bioreactor setup based on controlled inflation of tubing was used to achieve synchronized electromechanical stimulation. (a) Two solenoid valves controlled by computer regulated the tubing pressure and stretched the scaffold wrapped around the tubing; (b) Fibers wrapped around the silicone tubing remained aligned and attached closely to the surface of the tubing. The scaffold thickness used in this study was fixed at 50 μm; (c) Mechanical stimulation applied in this study was 1-h stimulation (stretched at 1 Hz) followed by 5-h rest. Electrical stimulation (20 V, 10 ms pulse width) was applied with the same stimulation regime. Synchronized stimulation regime was set at electrical stimulation commencing when mechanical stretching ceased.

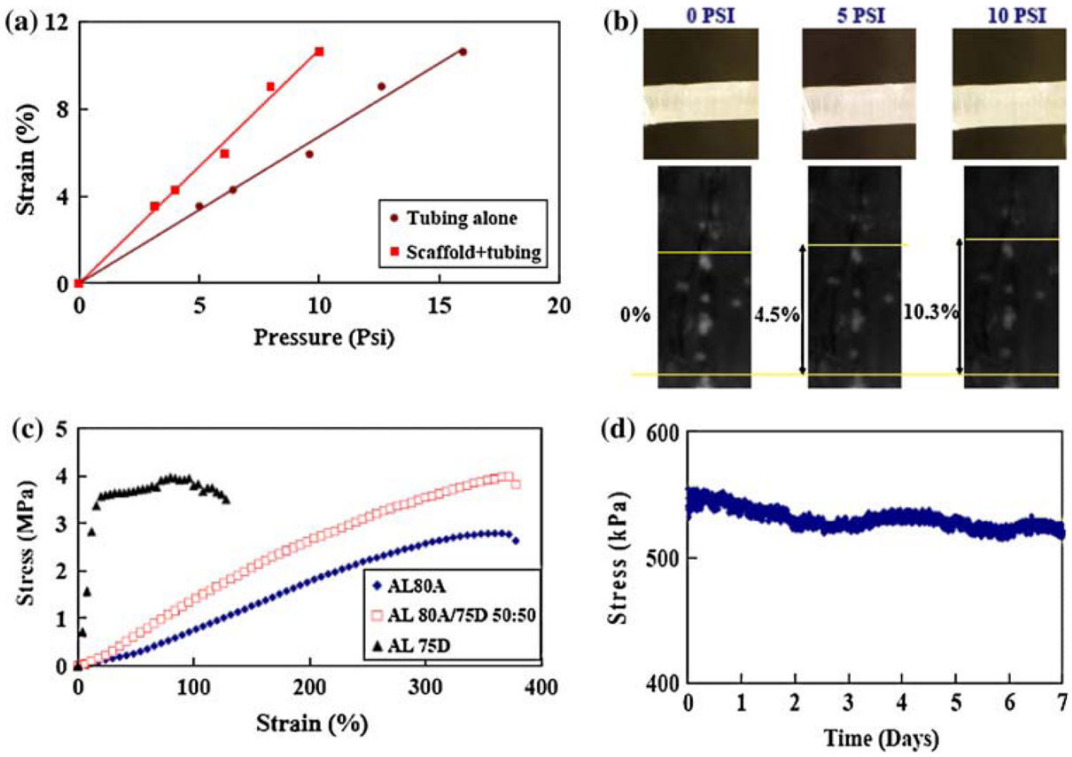

FIGURE 2.

(a) Measurement of strain in the tubings inflated as a function of pressure. Increase in pressure linearly correlated with the strain in the tubing. The attachment of aligned fibers around the silicone tubing shifted the strain–pressure curve left-ward, although it was still able to achieve at least 10% strain; (b) Fluorescent images of blue microspheres embedded on the nanofibers illustrated the microscopic displacement of the fibers as a result of tubing circumference change. The displacement between two clusters of microspheres over various pressures indicated that the strain rate measured by the diameter change would match the strain experienced by the fibers; (c, d) Mechanical properties of aligned fibers produced using polyurethane of different stiffness (80A, 55D and a 50:50 volume ratio blend). Fibers produced using 80A polyurethane were capable of stretch up to 300%, and remained mechanically stable under 10% cyclic strain at 1 Hz over 7 days. Yield stress of 80A fibers was around 2 MPa. Fibers produced using 55D polyurethane were more rigid, with yield elongation at 100% and similar breaking stress. Fibers produced using a 50:50 volume ratio blend have mechanical properties closer to 80A than 55D polyurethane.

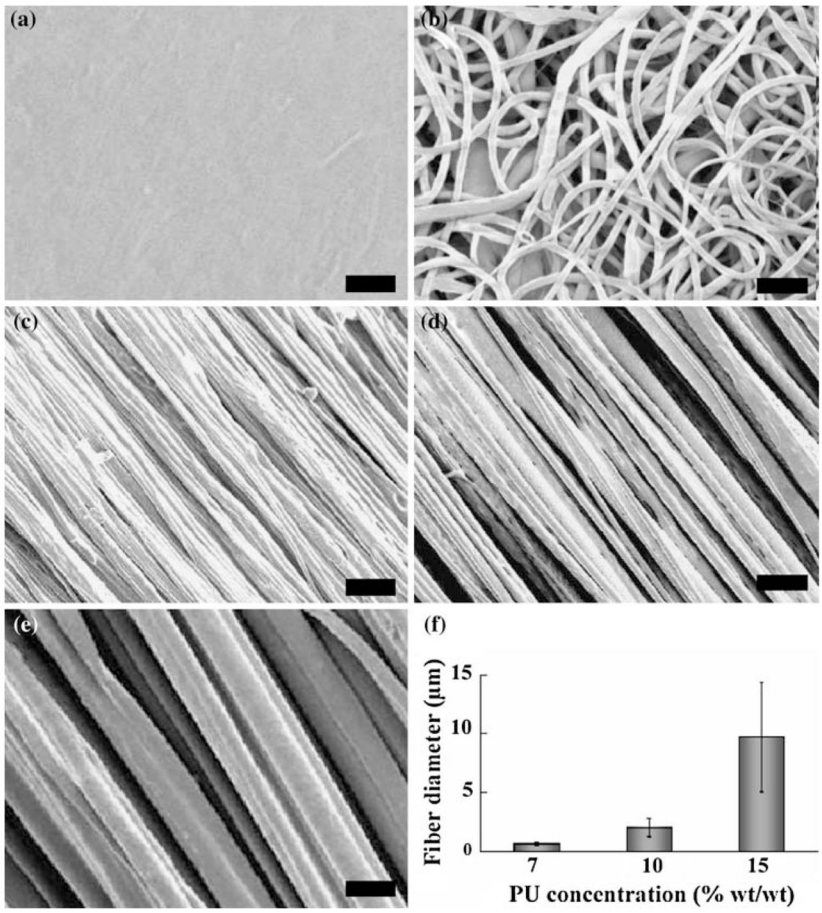

FIGURE 3.

SEM images of various topographical surfaces. (a) Film; (b) random fibers; (c) aligned nanofibers; (d) aligned 2 μm fibers; and (e) aligned 10 μm fibers. Scale bars are 5 μm in a–d and 10 μm in e; (f) Fibers of various diameters (600 nm, 2 μm and 10 μm) were produced by varying the concentration of the polyurethane solution.

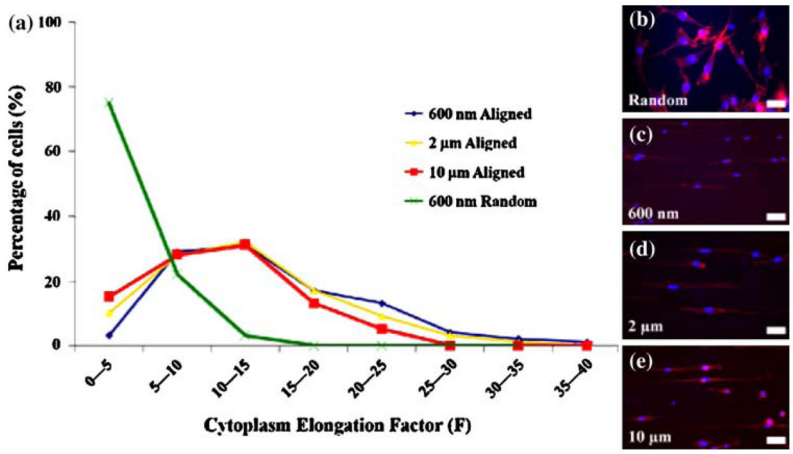

FIGURE 4.

Cell alignment and elongation on various topographical surfaces. (a) Morphology of myoblasts (seeding density = 5000 cells/cm^2) on random and aligned fibers was evaluated by measuring the cytoplasm elongation factor (defined as $F = (L - W)/W$, where L = length and W = width of cytoplasm). A minimum of 100 cells was measured for each group to achieve statistical significance; (b–e) Cells were randomly oriented and minimally aligned when cultured on random fibers but became more elongated on aligned fibers. Greater than 90% of the cells were oriented to the direction of the fiber within 10°. The cells were labeled with Alexa^{594} phalloidin and DAPI for their actin filaments and nuclei, respectively. Scale bars: 40 μm.

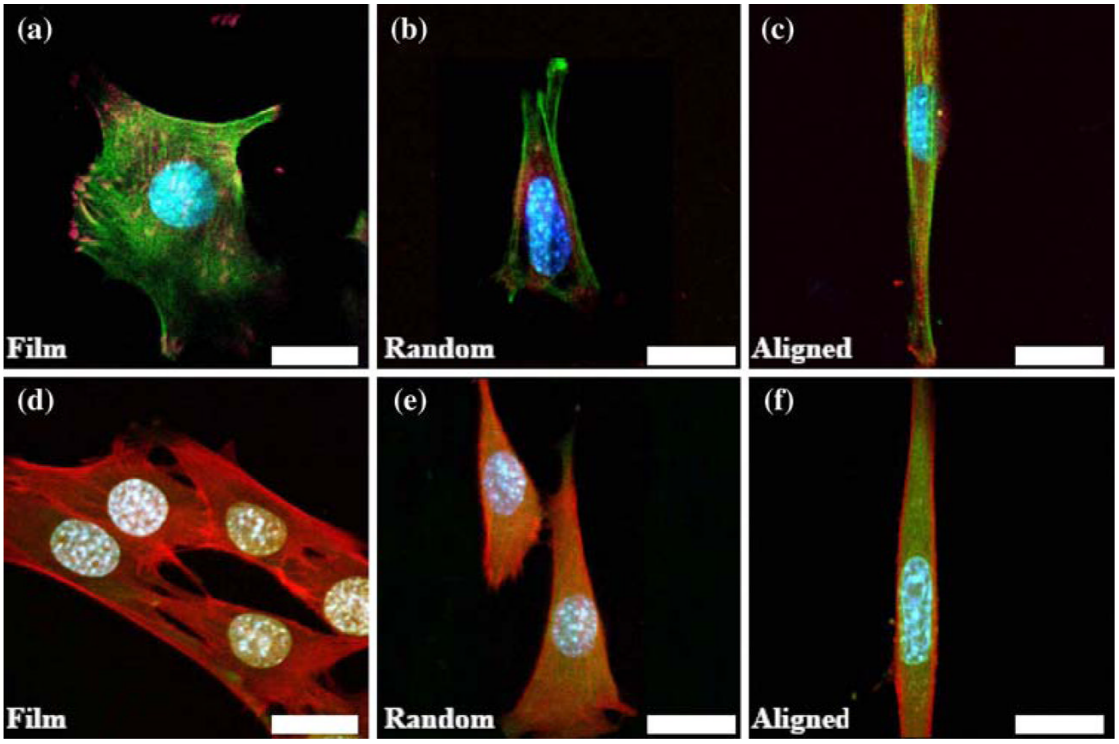

FIGURE 5.

Confocal images of focal adhesion sites and transient receptor potential cation channel-1. Immunofluorescent images of focal adhesion sites (red) and actin filaments (green) of myoblasts cultured on (a) film; (b) random; and (c) aligned fibers. Focal adhesion sites reorganized from the periphery of the cytoplasm towards the center of the cells when the myoblasts were cultured in aligned topography. (d–f) Confocal images of actin filaments (red) and TRPC-1 (green) demonstrated an upregulation of stretch activated cation channels in cells cultured on aligned fibers. Cell nuclei were stained blue with DAPI. Scale bar: 20 μm.

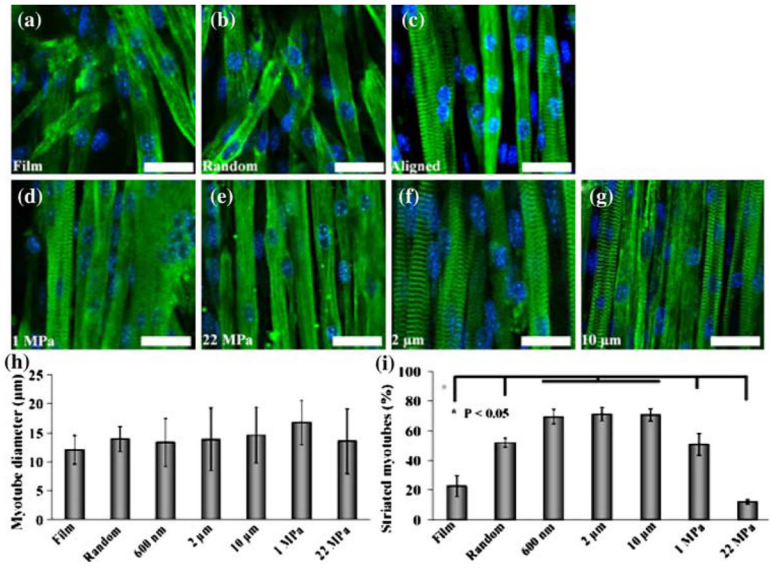

FIGURE 6.

Differentiation of myotubes on various topographical surfaces. Skeletal myoblasts cultured on various topographical surfaces were immunostained for α-actinin (green; blue = nuclei) to show striation. Myotubes were randomly oriented and less striated when cultured on (a) film and (b) random fiber surfaces; (c) When cultured on aligned PU fibers (600 nm with stiffness of 0.5 MPa), myotubes were highly aligned with 70% of myotubes showing striation; (d, e) The degree of striation decreased when myoblasts were cultured on stiffer aligned PU fibers (1 MPa and 22 MPa); (f, g) Degree of striation in the myotubes was comparable among the groups with fiber diameters of 600 nm to 10 μm; (h) Average myotube diameter did not significantly differ among various topographical surfaces, while (i) percentage of striated myotubes was dependent on topographical features and matrix stiffness. Scale bar: 20 μm.

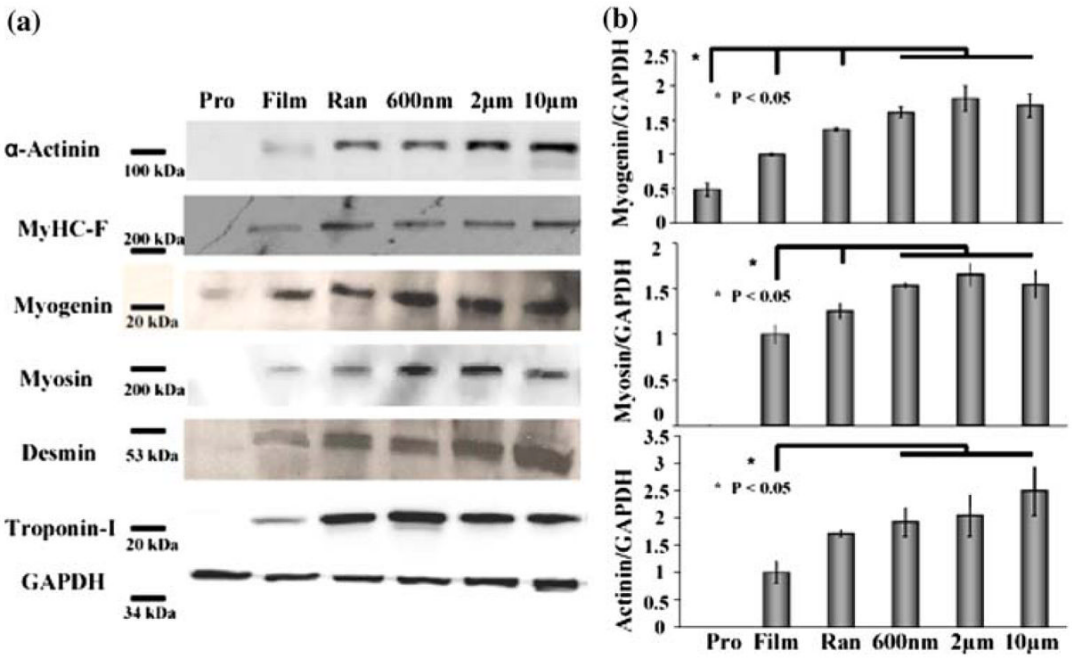

FIGURE 7.

Western blots of contractile proteins. (a) All contractile proteins were upregulated in myotubes cultured on aligned fibers compared to random fibers and film; (b) The upregulation of myosin, myogenin, and α-actinin was statistically higher in aligned fibers compared to random fibers and film samples. Western blotting analysis of myotubes cultured on different fiber sizes did not reveal significant difference among the groups. Values were normalized to GAPDH level.

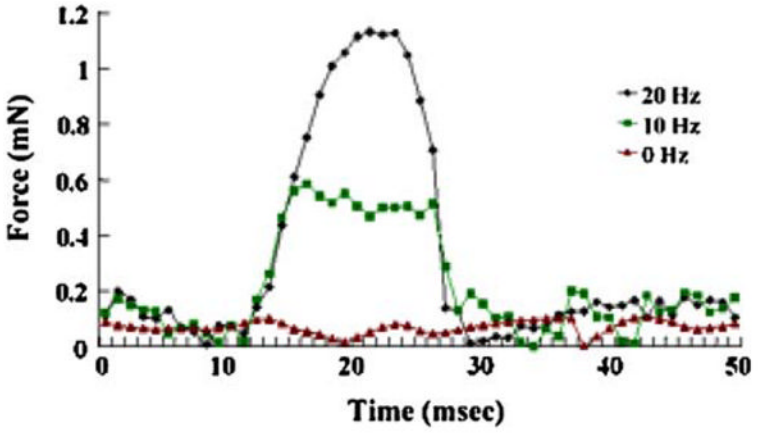

FIGURE 8.

Contractility measurement of myotubes cultured on aligned fibers. Contractility of the myotubes cultured on aligned fiber surface was measured at 14 days post-differentiation using a μN force transducer. The cell-fiber construct was stimulated for 15 ms starting at 10 ms time point and 20 V at various frequencies. The tetanus force measured was approximately 1 mN with an average time to tetanus around 10 ms.

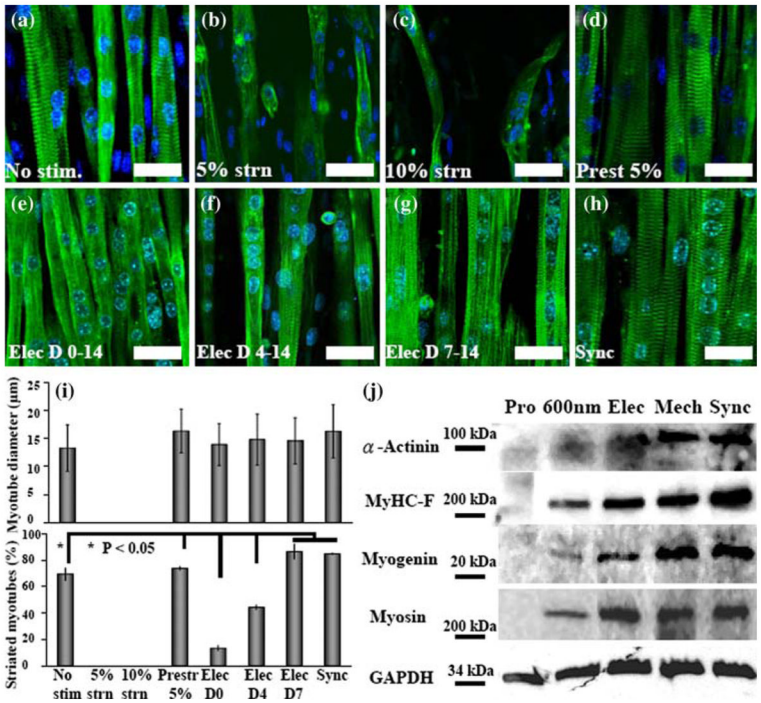

FIGURE 9.

Confocal images and Western blotting analysis of myotubes cultured under various stimulation regimes. Skeletal myotubes cultured under various stimulation regimes were immunostained for α-actinin (green; blue = nuclei) to show striation. (a–c) Application of 5 or 10% cyclic strain to cells cultured on aligned fibers resulted in overstretching and appeared to drive the myoblasts into proliferative instead of differentiative state; (d, i) Pre-stretching of the myoblasts before application of cyclic loading led to enhanced differentiation; (e, f, i) Electrical stimulation applied to the myotubes at earlier time points (Day 0 and 4 post-differentiation) showed detrimental effect in the development of striated myotubes; (g, i) When electrical stimulation was applied post-myotube assembly (day 7), it induced contraction and led to an increase in striation; (h, i) Cells cultured under synchronized stimulation showed insignificant increase in myotube diameter but significant increase in percent of striated myotubes; (j) Western blotting demonstrated an upregulation of contractile proteins mechanical, electrical or electromechanical stimuli was applied. There is a significant level of increase in fast myosin heavy chain when cells were cultured under synchronized stimulation. Scale bar: 20 μm.